Plasma tau-species positive neuron-derived extracellular vesicles in progressive supranuclear palsy

Yuanchu Zheng,[1,2,†] Huihui Cai,[1,2,†] Wenyi Kou,[3,†] Genliang Liu,[1,2] Yanlin Wang,[4] Jing Bai,[5] Yingshan Piao,[1,2] Xuedong Liu,[5] Xiaodong Zhu,[4] Jing Zhang,[6] Zhenwei Yu[7] and Tao Feng[1,2]

[†]**These authors contributed equally to this work.**

Abstract

The diagnosis of progressive supranuclear palsy (PSP) remains challenging, particularly in differentiating it from Parkinson's disease (PD) at early stages. Circulating neuron-derived extracellular vesicles (NDEVs) providing a peripheral window into central nervous system pathology may serve as promising biomarkers.

A total of 188 participants were recruited from 3 centers. A discovery cohort (40 PSP patients, 36 PD patients, and 31 healthy controls [HCs]) and a multicenter validation cohort (30 PSP patients, 27 PD patients, and 24 HCs) were established. NDEVs containing total tau, 4R tau, phosphorylated tau (ptau181, ptau217, ptau231 and ptau396) in plasma samples were analyzed using nano-scale flow cytometry. Multivariable logistic regression models were developed in the discovery cohort and strictly validated in the independent cohort using fixed model parameters.

In the discovery cohort, the concentrations of tau, 4R tau, ptau181, and ptau217-containing NDEVs in PSP patients were significantly higher than those in HCs and PD patients, while ptau396-containing NDEVs showed elevation exclusively in PSP compared to HCs. (PSP vs. HCs: P<0.001 for tau, P<0.001 for 4R tau, P<0.001 for ptau181, P=0.008 for ptau217, P=0.009 for ptau396; PSP vs. PD: P<0.001 for tau, P<0.001for4R tau, P=0.029 for ptau181, P=0.003 for ptau217). An integrated model incorporating these biomarkers achieved an area under the curve (AUC) of 0.965 (90.0% sensitivity, 96.8% specificity) for distinguishing PSP from HCs, and an AUC of 0.963 (87.5% sensitivity, 94.4% specificity) for distinguishing PSP from PD. In the validation cohort, the concentrations of tau, 4R tau, ptau181, ptau217, and ptau396-containing NDEVs in plasma were significantly higher in PSP patients compared to HCs (PSP vs. HCs: P<0.001 for tau, 4R tau, and ptau217, P=0.03

for ptau181, *P*=0.017 for ptau396). Similarly, the concentrations of tau, 4R tau, ptau181, and ptau217 were higher in PSP patients than in PD patients (PSP vs. PD: *P*<0.001 for tau, 4R tau, and ptau217, *P*=0.025 for ptau181). The integrated model yielded an AUC of 0.971 for distinguishing PSP from HCs and 0.990 for distinguishing PSP from PD. Notably, in early-stage patients, the integrated model achieved an AUC of 0.987 in differentiating early-stage PSP from PD.

These findings indicate that plasma tau-species-containing NDEVs are promising biomarkers for PSP, offering high sensitivity and specificity for distinguishing PSP from both HCs and PD, particularly in early disease stages. Further large-scale, longitudinal studies are warranted to fully validate these findings and explore their role in PSP pathophysiology and progression.

Author affiliations:

1 Center for Movement Disorders, Department of Neurology, Beijing Tiantan Hospital, Capital Medical University, Beijing, 100070, China

2 China National Clinical Research Center for Neurological Diseases, Beijing, 100070, China

3 Department of Neurology, Beijing Hospital, National Center of Gerontology, Institute of Geriatric Medicine, Chinese Academy of Medical Sciences, Beijing, 100730, China

4 Department of Neurology, Tianjin Medical University General Hospital, Tianjin, 300052, China

5 Department of Neurology, Xijing Hospital of Air Force Military Medical University, Xi'an, 710032, China

6 Department of Pathology, the First Affiliated Hospital and School of Medicine, Zhejiang University, Hangzhou, 310003, China

7 Beijing Neurosurgical Institute, Capital Medical University, Beijing, 100070, China

Correspondence to: Tao Feng

Center for Movement Disorders, Department of Neurology, Beijing Tiantan Hospital, Capital Medical University, Beijing, 100070, China

E-mail: bxbkyjs@sina.com

Correspondence may also be addressed to: Zhenwei Yu

Beijing Neurosurgical Institute, Capital Medical University, Beijing, 100070, China

E-mail: jasonyzw@163.com

Jing Zhang

Department of Pathology, the First Affiliated Hospital and School of Medicine, Zhejiang University, Hangzhou, 310003, China

E-mail: jzhang1989@zju.edu.cn

Running title: Neuron-derived tau containing EVs in PSP

Keywords: progressive supranuclear palsy; neuron-derived; extracellular vesicles; tau-species; biomarkers

Introduction

Progressive supranuclear palsy (PSP) is a tauopathy characterized by the predominant aggregation of 4-repeat (4R) tau isoforms.[1] Neuropathological features of PSP encompass the distinct morphology of tau aggregates in neurons, oligodendrocytes, and astrocytes, coupled with the specific neuroanatomical distribution of tau pathology and resultant neurodegeneration.[2] PSP presents with diverse clinical manifestations. Core clinical features include ocular motor dysfunction, postural instability, akinesia, and cognitive dysfunction.[3] Clinical predominance types are determined based on the combination of these features, including PSP-RS (Richardson's syndrome), PSP-OM (ocular motor), PSP-PI (postural instability), PSP-P (Parkinsonism), PSP-F (frontal), and PSP-PGF (pure akinesia with gait freezing), among others.[4,5] The diagnosis of PSP can be complicated due to the diverse clinical subtypes and symptom overlap with Parkinson's Disease (PD) and other atypical parkinsonian syndromes. This diagnostic complexity often results in a high rate of misdiagnosis, which impedes the development of disease-modifying treatments for PSP.[6,7] Therefore, there is an urgent need for reliable biomarkers that can facilitate early diagnosis and differentiate PSP from PD.

Previous studies have demonstrated the detection of tau species in biofluids and peripheral tissues of patients with PSP. These findings encompass a range of sample types, including plasma, olfactory and oral epithelium, and skin biopsies.[6,8-13] Notably, plasma serves as a routinely accessible clinical sample among these biospecimens. Recent advances in biomarker research have underscored the potential of plasma extracellular vesicles (EVs), particularly neuron-derived extracellular vesicles (NDEVs), as valuable tools for neurological diagnostics.[14-16] These NDEVs, capable of crossing the blood-brain barrier, transport proteins and nucleic acids that reflect the physiological and pathological state of CNS.[17,18]

Several studies have demonstrated that concentrations of total tau and phosphorylated tau proteins (ptau181, ptau217, ptau396) in EVs or NDEVs from the peripheral blood of Alzheimer's disease (AD) patients are significantly increased and can serve as diagnostic and progression-monitoring biomarkers for AD.[14,15,19,20] However, limited research has been conducted on the tau species in EVs or NDEVs in PSP. Meloni et al. found that concentrations of tau aggregates in serum NDEVs of PSP patients were significantly higher than those in PD patients.[21] This finding suggests that tau-species in NDEVs could potentially serve as biomarkers for PSP, offering a less-invasive method to assess the pathological state of the CNS. Currently, the levels of total tau, 4R tau, phosphorylated tau (ptau181, ptau217, ptau231 or ptau396) containing NDEVs in plasma in PSP are still unknown, highlighting the need for further investigation.

The objective of this study was to develop biomarkers based on plasma tau-species-containing NDEVs across two independent cohorts (discovery and validation) to differentiate PSP patients from PD patients and HCs. This study employed a nano-scale flow cytometry technique to directly identify and quantify NDEVs carrying tau species.[14,15,22,23] We used NMDAR2A as a hallmark for the analysis of plasma NDEVs, which has been demonstrated to provide high specificity and reliability.[15]

Materials and methods

Study design and participants

A total of 188 participants, comprising individuals with PSP, PD patients, and healthy controls (HCs), were recruited from Beijing Tiantan Hospital, Xijing Hospital of Air Force Military Medical University, and Tianjin Medical University General Hospital between January 2022 and March 2023. The single-center discovery cohort, consisting of 107 participants (40 with PSP, 36 with PD, and 31 HCs), was recruited from Beijing Tiantan Hospital between January 2022 and June 2022. The multicenter validation cohort

comprised 81 participants (30 with PSP, 27 with PD, and 24 HCs) recruited from the three sites between July 2022 and February 2023.

Clinical diagnosis of PSP and PD was made by physicians specialized in movement disorders, according to the Movement Disorder Society Clinical Diagnostic Criteria for PSP and PD.[3,24] Furthermore, the initial diagnoses were confirmed through clinical re-evaluation after a follow-up period of at least two years. Exclusion criteria for PD and PSP participants comprised other neurodegeneration disorders, severe head injury, a history of stroke, severe psychiatric disorders, and severe systemic disorders. Disease severity in PSP patients was assessed Movement Disorder Society Unified Parkinson's Disease Rating Scale Part Ⅲ (MDS-UPDRS Ⅲ). PSP was classified into the RS and non-RS subtypes.[3] PD patients underwent assessments using MDS-UPDRS Ⅲ and the Hoehn-Yahr scale during the OFF-medication period. Cognitive function was assessed using the Montreal Cognitive Assessment (MoCA) and the Mini-Mental State Examination (MMSE). HCs were excluded if they had a diagnosis of PD or other neurodegenerative disorders, a family history of movement diseases, severe head injury, a history of stroke, severe psychiatric disorders, severe respiratory disease, and severe heart disease.

The protocol for this cross-sectional study was reviewed and approved by the Ethics Committee of Beijing Tiantan Hospital, Capital Medical University (KY2022-190-03). All participants provided informed consent.

Plasma sample preparation

Venous blood samples were collected from fasting participants in the morning using ethylenediaminetetraacetic acid coated tubes. The blood samples were then centrifuged at 1500 × g for 15 min (4℃), and supernatant was then centrifuged at 12,000 × g for 30 minutes (4 ℃). The plasma supernatant was stored at −80℃ for nano-scale flow cytometry and nano-particle tracking analyses.

The reference plasma was pooled equally with plasma samples from 10 HCs. 2 mL of reference plasma was diluted with 2 mL 0.1-μm-filtered PBS and then centrifuged at 180,000 × g for 2 hours (4℃). Pellets were resuspended in 1 ml of filtered PBS and centrifuged again at 180,000 × g for 2 hours (4 ℃). The supernatant was carefully collected and pelleted EVs were then resuspended in 200 μL filtered PBS.

Neuron-derived EVs isolation

Neuron-derived EVs were isolated using an immunocapture protocol according to a previously established NDEVs isolation procedure. Briefly, Dynabeads M-270 Epoxy (Cat# 14311D, Invitrogen) were coupled with anti-NMDAR2A antibody (Cat# MA5-27693, Thermo Fisher Scientific) at a ratio of 10 μg antibody per 1 mg of beads, following the

manufacturer's antibody coupling kit protocol. These NMDAR2A-coated beads were utilized for both TEM sample preparation and western blot validation.

For TEM analysis, the total EV pellets obtained from ultracentrifugation were resuspended in PBS and incubated with the NMDAR2A-coated beads overnight at 4°C with gentle rotation. Following incubation, the bead-EV complexes were washed four times with PBS containing 0.1% BSA. The NDEVs were eluted from the beads by incubation in 70 µL of glycine buffer (0.1 M, pH 3.0) for 15 minutes, followed by neutralization with 15 µL of Tris-buffer (1 M, pH 7.0).

For western blot validation, immunoprecipitation was performed on raw plasma and EV-depleted plasma (supernatant after ultracentrifugation). Samples were incubated with the NMDAR2A-coated beads overnight at 4°C with gentle rotation. As a non-specific binding control, raw plasma was incubated with anti-FLAG Magnetic Beads (Cat# FNM-25-1000, Lablead) under identical conditions.

Transmission electron microscopy analysis

A volume of 5 µL of NDEV suspension was placed onto a copper grid coated with a carbon support film. The sample was incubated for 60 seconds, and any excess was removed using filter paper. The grid was then stained with a 2% uranyl acetate solution for 60 seconds. Excess uranyl acetate solution was removed with filter paper, and the sample was allowed to air-dry. Electron microscopy images were captured using a Tecnai F20 transmission electron microscope operating at 200 kilovolts.

Western blot analysis

The immunoprecipitated bead complexes were washed three times with PBS containing 0.1% BSA and proteins were eluted by boiling in Laemmli sample buffer for 10 minutes. Protein samples were separated on 4-20% Bis-Tris gels (Cat#M42010C, Genscript) and electrotransferred onto nitrocellulose membranes. After blocking with 5% non-fat milk, the membranes were incubated overnight at 4°C with the following primary antibodies: anti-NMDAR2A (Cat# ab174636, Abcam, 1:200 dilution), anti-L1CAM (Cat# 371608, BioLegend, 1:1000 dilution), anti-4R-tau (Cat# ab218314, Abcam, 1:2000 dilution), anti-Alix (Cat# 12422-1-AP, Proteintech, 1:1000 dilution), and anti-CD63 (Cat# 52090S, Cell Signaling Technology, 1:1000 dilution).

Nanoparticle tracking analysis

Two µL plasma samples from 10 patients with PSP, 10 patients with PD, and 10 HCs were diluted at a 1:500 ratio in PBS (pH 7.4). These diluted samples were then analyzed using the

ZetaView platform (Particle Metrix) to assess the distribution and concentration of nanoparticles.

NDEVs analysis with Cytoflex nano-scale flow cytometry

Utilizing Zenon IgG labeling kits, fluorophore conjugation was performed on antibodies following the manufacturer's guidelines. Specifically, the anti-NMDAR2A antibody (Cat# MA5-27693, Thermo Fisher Scientific) was labeled with Zenon Alexa Fluor 405 mouse IgG2b labeling kit (Cat# Z25213, Thermo Fisher Scientific). The anti-tau antibody (Cat# ab109392, Abcam) was labeled with Zenon Alexa Fluor 488 rabbit IgG labeling kit (Cat# Z25302, Thermo Fisher Scientific). The anti-4R tau antibody (Cat# ab218314, Abcam) and the phospho-tau (Thr217) antibody (Cat# 51625S, Cell Signaling Technology) were labeled with Zenon Alexa Fluor 647 rabbit IgG labeling kit (Cat# Z25308, Thermo Fisher Scientific). The phospho-tau (Thr181) antibody (Cat# MN1050, Thermo Fisher Scientific) and the phospho-tau (Thr231) antibody (Cat# 44-746G, Thermo Fisher Scientific) were labeled with Zenon Alexa Fluor 488 mouse IgG1 labeling kit (Cat# Z25002, Thermo Fisher Scientific). The phospho-tau (Ser396) antibody (Cat# 35-5300, Thermo Fisher Scientific) was labeled with Zenon Alexa Fluor 647 mouse IgG2b labeling kit (Cat# Z25208, Thermo Fisher Scientific). For the quantitative analysis of NDEVs, we employed a direct immunolabeling protocol on plasma samples without prior bead-based isolation. Five µL of plasma was placed in a flow cytometry tube. Then, 0.1 µg of fluorescent-conjugated NMDAR2A antibody was added and incubated for 30 minutes, followed by 0.2 µg of fluorescent-conjugated tau antibody for 20 minutes, all under light-protected conditions at room temperature.

Following incubation, the mixture was diluted 1:60 with PBS, vortexed, and centrifuged for 10 seconds. Quantitative detection was performed on the Cytoflex S platform (Beckman Coulter, Milano, Italy) using nano-scale flow cytometry in VSSC-H mode for vesicles below 500 nm, following our previously established method.[23] Gates were set using immunoglobulin isotype and blank controls. Double-positive events (NMDAR2A+ combined with tau, 4R tau, ptau181, ptau217, ptau231, or ptau396) were identified, and concentrations were calculated utilizing the volumetric sample injection feature of the Cytoflex S platform, which allows for direct particle counting per unit volume without the use of reference beads. The concentration (events/mL) was calculated based on the number of acquired events divided by the precise analyzed volume, adjusted for the PBS dilution factor. Controls were labeled at the same final antibody concentrations. The assay reproducibility was validated using pooled reference plasma analyzed in triplicate. The intra-assay coefficients of variation (CVs) for all measured Tau species were consistently <6% (range: 0.69% - 5.76%). To minimize inter-assay variability, samples from both cohorts were analyzed in a single continuous batch for each specific biomarker independently within 4 hours.

To assess the specificity of the NDEV identification, parallel double-labeling assays were performed using a recombinant rabbit monoclonal antibody against epithelial cell adhesion molecule (EpCAM) (Cat# ab308057, Abcam) under identical conditions to the NMDAR2A labeling. Plasma samples were pooled (n=5 pools per group) to ensure robust detection of rare events. Samples were co-stained with fluorophore-conjugated anti-Tau (or anti-4R-tau) antibodies and either anti-NMDAR2A or anti-EpCAM antibodies. During analysis, double-positive events were gated and their concentrations were quantified and compared between groups.

Statistical analysis

Statistical analyses were performed using GraphPad Prism 10 and Python 3.10. Group differences in biomarker concentrations were assessed using the Kruskal-Wallis test followed by Dunn's post hoc test. Associations between biomarkers and clinical indicators in the PSP group were evaluated using Spearman or Pearson correlation, with P-values adjusted for the false discovery rate (FDR) using the Benjamini-Hochberg method. To ensure comparability across biomarkers, concentrations were standardized to Z-scores based on the means and standard deviations of the discovery cohort (Supplementary Table S1). Multivariable logistic regression (Enter method) was employed to construct diagnostic models for distinguishing PSP from HCs and PD in the discovery cohort. These models were then externally validated in the independent validation cohort and early-stage subgroup by applying the fixed model parameters. Diagnostic performance was evaluated using receiver operating characteristic (ROC) curves, with the area under the curve (AUC), sensitivity, and specificity reported. All tests were two-tailed, with statistical significance set at $P < 0.05$.

Results

Demographic and Clinical Features

The demographic and clinical data of PSP patients, PD patients, and control subjects in both the discovery and validation cohorts are summarized in Table 1.

The discovery cohort from Beijing Tiantan Hospital included 40 PSP patients (18 RS and 22 non-RS) with a median disease duration of 3 years (range: 0.5-10 years), 36 PD patients with a median disease duration of 6 years (range: 1-16 years), and 31 control subjects. The multicenter validation cohort included 30 PSP patients (14 RS and 16 non-RS) with a median disease duration of 3 years (range: 0.83-8 years), 27 PD patients with a median disease duration of 5 years (range: 1-13 years), and 24 control subjects. In both cohorts, the

ages and genders of PSP patients, PD patients, and HCs were matched. In both cohorts, PSP patients showed greater cognitive impairment than PD patients. In the validation cohort, PSP patients exhibited higher MDS-UPDRS Ⅲ scores than PD patients, whereas no significant difference was observed in the discovery cohort.

Characteristics of EVs

TEM analysis visualized the anti-NMDAR2A-enriched NDEVs with an approximate diameter of 100 nm (Figure 1A). Western blot analysis demonstrated that anti-NMDAR2A immunoprecipitates from raw plasma contained NMDAR2A and L1CAM, two specific neuronal EV markers, along with general EV markers (Alix, CD63) and 4R-tau. Notably, these markers were either absent or markedly reduced in the IgG control (anti-flag) and in the EV-depleted plasma NMDAR2A-IP fractions (Figure 1B). NTA analysis indicated a broad peak centered around 100 nm (Figure 1C-1E) across the PD, PSP, and HC groups. No significant difference in EV concentration was observed among these groups (Figure 1F).

NDEVs analysis with Cytoflex nano-scale flow cytometry

We first quantified the absolute concentration of total NDEVs (NMDAR2A+ events) in the discovery cohort. The analysis revealed no significant differences in NDEV concentration across the HC, PSP, and PD groups (Supplementary Figure S1).

Subsequently, the concentrations of NDEVs containing tau, 4R tau, ptau181, ptau231, and ptau396 were compared between reference plasma and EV-depleted plasma samples, using normal IgG serving as an isotype technical control (Figure 2A-2L). To ensure the accuracy of EV measurement, a linearity dilution strategy was employed. Specifically, reference plasma labeled with tau species and NMDAR2A antibodies was diluted at ratios of 1:120, 1:240, and 1:480 in PBS and analyzed using the Cytoflex S platform (Figure 2M-2R).

To confirm the neuronal specificity of our EV identification strategy, we performed parallel double-labeling flow cytometry using the EpCAM antibody as a non-neuronal negative control. As shown in Supplementary Figure S2, we compared the concentration of EVs co-expressing Tau species with either NMDAR2A or EpCAM. The abundance of Tau+ NMDAR2A+ and 4R tau+ NMDAR2A+ events was markedly higher than that of Tau+ EpCAM+ and 4R tau+ EpCAM+ events. Furthermore, while the Tau+ NDEV and 4R-Tau+ NDEV populations showed significant elevation in PSP patients compared to HC and PD ($P < 0.05$), the Tau+ EpCAM+ EVs and 4R-Tau+ EpCAM+ EVs showed no significant differences across the groups, supporting the specificity of neuronal tauopathy in PSP patients.

Tau-species-containing NDEVs measurements in the discovery cohort

In the discovery cohort, the concentrations of tau, 4R tau, ptau181, and ptau217-containing NDEVs in plasma of PSP individuals were significantly higher than those in HCs and PD patients, ptau396-containing NDEVs were significantly elevated in PSP plasma versus HCs (PSP vs. HCs: $P_{tau} < 0.001$, $P_{4R\,tau} < 0.001$, $P_{ptau181} < 0.001$, $P_{ptau217} = 0.008$, $P_{ptau396} = 0.009$; PSP vs. PD: $P_{tau} < 0.001$, $P_{4R\,tau} < 0.001$, $P_{ptau181} = 0.029$, $P_{ptau217} = 0.003$; Kruskal-Wallis test with Dunn's multiple comparisons test, Figure 3A-3D, 3F). While ptau231-containing NDEVs showed comparable levels between PSP and PD or HCs, ptau396-containing NDEVs exhibited no significant differential expression specifically between PSP and PD. (Figure 3E-3F).

The ratios of tau-species positive NDEVs to tau-species positive EVs (referred to as ratio) were also analyzed. The ratio of tau-positive NDEVs to tau-positive EVs in patients with PSP was significantly higher than those in patients with PD ($P < 0.001$) and HCs ($P < 0.001$) (Figure 3G). Additionally, the ratio of 4R tau-positive NDEVs to 4R tau-positive EVs in patients with PSP was higher than those in patients with PD ($P = 0.001$) (Figure 3H), and the ratio of ptau231-positive NDEVs to ptau231-positive EVs in patients with PSP was higher than those in HCs ($P < 0.001$) (Figure 3K). There were no significant differences in other ratios achieved among PSP, PD, and HC groups (Figure 3I, 3J, 3L).

ROC analyses assessed the diagnostic utility of tau, 4R tau, ptau181, ptau217, ptau231, and ptau396-containing NDEVs in plasma for distinguishing PSP patients from HCs. The area under the curve (AUC) of ROC for these biomarkers were as follows: tau, 0.906 (95% CI 0.838-0.974); 4R tau, 0.761 (95% CI 0.650-0.872); ptau181, 0.785 (95% CI 0.681-0.889); ptau217, 0.691 (95% CI 0.568-0.813); ptau231, 0.625 (95% CI 0.495-0.755); and ptau396, 0.694 (95% CI 0.569-0.818) (Figure 3M). Additionally, a multivariate logistic regression model incorporating these tau-species-containing NDEVs yielded an AUC of 0.965 (95% CI 0.923-1.000), demonstrating a sensitivity of 90.0% and a specificity of 96.8% in differentiating PSP patients from HCs (Figure 3N).In distinguishing PSP from PD, the AUC values for these NDEVs were presented in Figure 3O: tau, 0.867 (95% CI 0.786-0.947); 4R tau, 0.818 (95% CI 0.726-0.910); ptau181, 0.668 (95% CI 0.545-0.791); ptau217, 0.721 (95% CI 0.607-0.835); ptau231, 0.590 (95% CI 0.461-0.719); and ptau396, 0.544 (95% CI 0.412-0.675). The corresponding multivariate logistic regression model, integrating these biomarkers, achieved an AUC of 0.963 (95% CI 0.925-1.000), with a sensitivity of 87.5% and specificity of 94.4% in differentiating patients with PSP from those with PD (Figure 3P). The detailed parameters of these fixed logistic regression models, including regression coefficients, *P* values, and odds ratios, are presented in Table 2.

To evaluate whether the NMDAR2A-based identification strategy provides superior diagnostic value compared to analyzing total circulating EVs, we further quantified the concentration of tau-species-containing EVs (without NMDAR2A gating) in the discovery cohort (Supplementary Figure S3). Although tau-species-containing EVs showed differences in certain comparisons among groups, their diagnostic efficacy was inferior to that of NDEVs. Specifically, the integrated model based on tau-species-containing EVs achieved an AUC of 0.842 for distinguishing PSP from PD, which was lower than that of the NDEV-based model. Notably, the NDEV-based strategy substantially improved the specificity for differentiating PSP from PD (94.4%) compared to the total EV strategy (72.2%), confirming that the specific analysis of the neuron-derived subpopulation is essential for maximizing diagnostic accuracy.

Tau-species-containing NDEVs measurements in the validation cohort

In the multicenter validation cohort, the concentrations of tau, 4R tau, ptau181, ptau217, and ptau396-containing NDEVs in plasma were significantly higher in PSP patients compared to HCs ($P_{tau} < 0.001$, $P_{4R\,tau} < 0.001$, $P_{ptau181} = 0.030$, $P_{ptau217} < 0.001$, $P_{ptau396} = 0.017$). Similarly, concentrations of tau, 4R tau, and ptau181-containing NDEVs were higher in PSP patients than in PD patients ($P_{tau} < 0.001$, $P_{4R\,tau} < 0.001$, $P_{ptau181} = 0.025$, $P_{ptau217} < 0.001$) (Figure 4A-4F).

The ratio of tau-positive NDEVs to tau-positive EVs in patients with PSP was significantly higher than those in PD patients ($P = 0.002$) and HC ($P < 0.001$). Additionally, the ratio of 4R tau-positive NDEVs to 4R tau-positive EVs in PSP patients was higher than those in PD patients ($P = 0.046$), and the ratio of ptau231-positive NDEVs to ptau231-positive EVs in PSP patients was higher than those in HCs ($P < 0.001$). The ratio of ptau396-positive NDEVs to ptau396-positive EVs in PSP patients was higher than those in PD patients ($P = 0.032$). The ratio of ptau231-positive NDEVs to ptau231-positive EVs showed no significant differences among PSP, PD, and HC groups (Figure 4G-4L).

To assess the generalizability of our diagnostic approach, we applied the fixed logistic regression model parameters derived from the discovery cohort (Table 2) directly to the independent validation cohort. ROC analyses of the individual tau-species-containing NDEVs for differentiating PSP patients from HCs and PD patients are shown in Figures 4M and 4O, respectively. By applying the fixed integrated model, we achieved an AUC of 0.971 (95% CI 0.919–1.000), with a sensitivity of 100.0% and specificity of 91.7%, for distinguishing PSP patients from HCs (Figure 4N). Furthermore, this fixed model validated with an impressive AUC of 0.990 (95% CI 0.973–1.000), yielding a sensitivity of 96.7% and a specificity of 96.3%, for distinguishing patients with PSP from those with PD (Figure 4P).

Tau-species-containing NDEVs in early-stage PSP vs early-stage PD

To evaluate the potential of tau-species-containing NDEVs as early diagnostic markers for PSP, we compared the concentrations of tau-species-containing NDEVs between 43 early-stage PSP patients and 18 early-stage PD patients, both with a disease duration of three years or less.[25] The demographic and clinical data are summarized in Table 3.

Total tau-, 4R tau-, and ptau217-containing NDEVs were significantly elevated in PSP compared to PD ($P_{tau} < 0.001$, $P_{4R\,tau} < 0.001$, $P_{ptau217} < 0.001$), suggesting their potential utility in distinguishing PSP from PD at early clinical stages (Figure 5A-5F). ROC analyses of tau-species-containing NDEVs for distinguishing early-stage PSP and early-stage PD patients are shown in Figure 5G. The integrated model incorporating these NDEVs achieved an AUC of 0.987 (95% CI: 0.964–1.000), with a sensitivity of 95.3% and a specificity of 94.4% in differentiating early-stage PSP from early-stage PD (Figure 5H).

Correlations of tau-species-containing NDEVs with clinical characteristics

To explore the clinical significance of tau-species-containing NDEVs in PSP patients, we analyzed the correlations between these biomarkers and demographic and clinical characteristics, such as age, disease duration, MMSE, MoCA, and MDS-UPDRS-III scores. No correlations remained statistically significant after adjusting for multiple comparisons using the FDR correction (adjusted $P > 0.05$). The differences between PSP subtypes were also compared, but no significant differences were observed in the levels of tau-species-containing NDEVs between the PSP-RS and PSP-non-RS groups (Supplementary Figure S4).

Discussion

In this study, we used nano-scale flow cytometry to quantify NDEVs containing total tau, 4R tau, ptau181, ptau217, ptau231 and ptau396 in plasma, aiming to discover reliable plasma biomarkers for PSP. These biomarkers effectively differentiated PSP from PD and control subjects across two cohorts, encompassing a total of 188 participants (70 PSP patients, 63 PD patients, and 55 HCs). Our findings indicate significantly increased tau-species-containing NDEV concentrations in plasma samples of PSP patients, offering an approach to early and accurate diagnosis. The multicentral validation across 3 independent cohorts underscores the significance and potential clinical utility of these biomarkers.

Diagnosing PSP, particularly in its early stages, presents a clinical challenge due to its overlap with PD. Numerous studies have focused on the development of peripheral tissue

and fluid-based biomarkers for PSP diagnosis. The measurement of total tau and phosphorylated tau in cerebrospinal fluid (CSF) offers some diagnostic utility.[26,27] Recent applications of 4R-tau Seed Amplification Assay (SAA) techniques to CSF and skin samples show great promise.[28,29] However, CSF and skin biopsies are invasive and have limited practicality for early screening, underscoring the need to develop minimally invasive yet precise biomarkers in readily accessible biofluids like plasma. Among other biofluids and peripheral tissues, blood is a routinely accessible clinical sample. Recent studies highlighted the potential of blood-derived NDEVs, especially in neurological diagnostics.[14-16] Meloni and colleagues[21] found that concentrations of tau aggregates in serum NDEVs of PSP patients were significantly higher than those in PD patients, utilizing an immunocapture assay combined with an ELISA approach to quantify pathological tau aggregates. To date, only one study[21] has examined tau aggregates in blood NDEVs of PSP patients, while other disease-relevant tau species, such as total tau, 4R tau, and hyperphosphorylated isoforms, have not been investigated in peripheral NDEVs. In this study, diverging from prior methodologies, we employed nano-scale flow cytometry to measure total tau, 4R tau, and a series of phosphorylated tau species-containing NDEVs, providing a comprehensive assessment. We developed and validated plasma tau-species-containing NDEVs as biomarkers for differentiating PSP patients from PD patients and HCs, demonstrating high diagnostic accuracy and making this method valuable for clinical and research applications.

PSP is a neurodegenerative disorder characterized by the pathological deposition of tau protein in the CNS.[1,30] Postmortem neuropathological studies have confirmed accumulation of hyperphosphorylated tau aggregates forming neurofibrillary tangles in neurons and astrocytic pathologies in PSP brains.[31] Previous investigations have demonstrated significantly elevated tau concentrations in the CSF of PSP patients.[27,32,33] In this study, nano-scale flow cytometry revealed that the levels of NDEVs carrying total tau, 4R tau, ptau181, and ptau217 in plasma were significantly higher in both discovery and validation cohorts of PSP patients compared to those in HCs and PD patients, which demonstrates that the tau species carried by peripheral NDEVs may objectively reflect CNS tau pathological burden. Notably, we observed significant elevations in NDEVs containing ptau181 and ptau217. While these epitopes are widely recognized as core biomarkers for AD, their elevation in PSP suggests that phosphorylation at Thr181 and Thr217 is not exclusive to AD pathology but also occurs in 4R-tauopathies. Although their diagnostic performance was distinct from the primary 4R-tau pathology, these markers proved critical in differentiating PSP from PD. This is likely because PD is a synucleinopathy characterized by minimal tau burden, whereas PSP involves extensive tau hyperphosphorylation. The robust contribution of ptau217 to our multivariate model (PSP vs. PD) further underscores

its utility in capturing the broader spectrum of tau hyperphosphorylation to exclude non-tau movement disorders.

From a pathophysiological perspective, NDEVs can traverse the BBB bidirectionally. Tau protein can be actively transported from the CNS to peripheral circulation via NDEVs. Critically, neuron-derived tau accumulation has been shown to induce BBB disruption,[34] establishing a positive feedback loop that exacerbates tau pathology propagation. These findings collectively underscore the dual role of peripheral NDEVs as non-invasive biomarkers reflecting central tau pathology and dynamic carriers of pathogenic tau species.

While L1CAM has traditionally been utilized as a marker of NDEVs, recent investigations have raised concerns regarding its specificity. Notably, evidence suggests that a significant fraction of L1CAM in plasma exists as a soluble protein rather than being EV-associated, and its expression is not exclusively restricted to the central nervous system.[35] While recent single-EV analyses have reinforced the validity of L1CAM as a neuronal marker,[36] the persistence of conflicting evidence regarding the ratio of soluble versus EV-bound L1CAM necessitates caution.[37] To mitigate these potential confounders, we employed NMDAR2A as the capture target in the present study, consistent with previous investigations.[15,38] As an integral transmembrane protein highly enriched at postsynaptic densities, NMDAR2A offers a robust alternative for isolating NDEVs with high neuronal specificity, thereby ensuring that the analyzed tau species are predominantly of neuronal origin.[15]

In this research, plasma NDEVs were assessed using nano-scale flow cytometry, a recently developed assay that enables the direct measurements of the fluorescence-labeled EVs in biofluids without the requirement of EV pre-immunoprecipitation. Critically, prior studies relying on immunocapture-ELISA workflows exclusively quantify aggregated tau, overlooking the diagnostic potential of distinct tau isoforms and phosphorylation-specific epitopes within NDEVs. Moreover, conventional immunocapture-ELISA methods require multistep workflows—including vesicle isolation, target capture, and enzymatic signal amplification—which increase sample volume requirements and prolong processing time. In contrast, our nano-scale flow cytometry-based approach minimized sample consumption while accelerating time-to-result. This methodological advancement enables scalable, high-throughput screening—a critical advantage for clinical translation. Prior studies[21] reported an AUC of 0.908 for distinguishing PSP from PD using tau aggregates in serum NDEVs, whereas our approach achieved superior discriminative power, with AUCs of 0.963 (discovery cohort), 0.990 (validation cohort), and 0.987 (early-stage). The nano-scale flow cytometry technique employed in this study offers a streamlined, direct

detection approach that enhances diagnostic efficacy. This efficiency makes it a valuable method for broader applications in both clinical and research environments.

Despite the clear differentiation observed between groups, the technical nature of the high-intensity signals in flow cytometry warrants discussion. As observed in Figure 2, reference plasma samples exhibited high-intensity signals following a diagonal distribution between markers. We acknowledge that this high fluorescence intensity may reflect a composite signal involving both biological antigen abundance and secondary antibody clustering events. It is possible that at high labeling concentrations, antibodies may undergo nucleation around the antigen-bound EV surface, creating an amplification effect that enhances fluorophore density. Crucially, however, this phenomenon appears to be strictly antigen-dependent. As evidenced by the IgG isotype controls, non-specific binding was minimal, and the high-intensity diagonal patterns were not observed in the absence of the specific target antigen. This suggests that while the signal quantification may not be strictly stoichiometric (1:1), the assay effectively retains the specificity required to distinguish biomarker abundance between cohorts. Thus, this mechanism may inadvertently serve as a sensitivity booster, facilitating the detection of NDEVs that might otherwise fall below the detection threshold of conventional flow cytometry, thereby supporting the robust group differences observed in our study.

This study has several strengths. Firstly, we measured total tau, 4R tau, and a series of phosphorylated tau species-containing NDEVs, providing a comprehensive measurement that has not been thoroughly analyzed in prior research. The anti-4R tau antibody (Cat# ab218314) used in our analysis is highly specific for 4R tau isoforms with minimal cross-reactivity to 3R tau, ensuring the pathological relevance of this key biomarker. Secondly, our research leverages two robust cohorts that encompass a broad spectrum of disease stages, enhancing the representativeness and applicability of our findings. The discovery cohort and a multicenter validation cohort include both early and advanced cases of PSP, ensuring that our biomarkers are tested across the full trajectory of the disease. This diversity facilitates the generalizability of our results and demonstrates the utility of our biomarkers in the early stage of the disease when differential diagnosis is difficult. This stability across disease stages strongly supports their use as diagnostic biomarkers; however, it also implies that these specific markers may be less suited for tracking disease progression or for monitoring therapeutic response in clinical trials. Thirdly, the study employs state-of-the-art nano-scale flow cytometry for the analysis of NDEVs, which allows easy and precise quantification of tau-species. This advanced methodology ensures high sensitivity and specificity in biomarker detection, making it a potential standard in clinical diagnostic processes.

There are several limitations to our study that warrant consideration. Firstly, while the clinical diagnoses were made according to the latest Movement Disorder Society criteria, known for their high specificity and sensitivity, the absence of pathological confirmation of PSP introduces a potential degree of diagnostic uncertainty. Secondly, the cross-sectional nature of this study limits our ability to observe the progression of the disease over time. Longitudinal studies would be valuable in addressing these aspects by following individuals throughout the course of the disease. Thirdly, while we identified elevated levels of multiple tau species within NDEVs (including total tau, 4R tau, and phosphorylated isoforms), the mechanisms underlying this selective enrichment of pathological tau in NDEVs remain speculative. Potential explanations—such as aberrant neuronal secretion, impaired vesicle clearance—require validation through dedicated mechanistic studies.

In conclusion, our research underscores the promising potential of tau-species-containing NDEVs in plasma as robust biomarkers for PSP. Our analysis, conducted across discovery and multicenter validation cohorts, consistently demonstrated that these biomarkers provide high specificity and sensitivity in differentiating PSP from PD and HCs. The quantification of tau, 4R tau, and phosphorylated tau-positive NDEVs, facilitated by advanced nano-scale flow cytometry, represents a significant advance in the non-invasive diagnosis of PSP. Importantly, the utility of these biomarkers in clinical settings is highlighted by their ability to enhance diagnostic accuracy in the early stages of the disease, when traditional clinical assessments may still be inconclusive. The findings from this study not only support the integration of tau-species-containing NDEVs into routine diagnostic protocols, but also emphasize their potential role in stratifying patients in clinical trials aimed at exploring disease-modifying therapies. Moving forward, the essential next steps are to: (i) validate these NDEV biomarkers in large, prospective, longitudinal cohorts; (ii) test their specificity against other neurodegenerative conditions, particularly other 4R tauopathies like Corticobasal Degeneration and α-synucleinopathies like Multiple System Atrophy; and (iii) directly compare the diagnostic performance of this NDEV panel against other leading fluid biomarkers, such as plasma NfL, GFAP, and CSF tau markers, within the same patient cohorts. Such research will be crucial for establishing their role in the clinical diagnostic pathway and for patient stratification in future therapeutic trials.

Data availability

The data that support the findings of this study are available from the corresponding author, upon reasonable request.

Acknowledgements

We deeply appreciate the participants for their generous donation of samples.

Funding

This research was funded by the National Natural Science Foundation of China (Grant Numbers 82501504, U24A20694, 82401480, 82271459, and 82020108012), the Beijing Municipal Natural Science Foundation (Grant Numbers 7232013, and 7244331), the China Postdoctoral Science Foundation (Grant Number 2024T170593), the funding from Beijing Neurosurgical Institute (Grant Number 11000025T000003319495-3), and the Beijing Postdoctoral Research Foundation.

Competing interests

The authors report no competing interests.

Supplementary material

Supplementary material is available at *Brain* online.

References

1. Stamelou M, Respondek G, Giagkou N, Whitwell JL, Kovacs GG, Hoglinger GU. Evolving concepts in progressive supranuclear palsy and other 4-repeat tauopathies. *Nat Rev Neurol*. Oct 2021;17(10):601-620. doi:10.1038/s41582-021-00541-5

2. Forrest SL, Lee S, Nassir N, et al. Cell-specific MAPT gene expression is preserved in neuronal and glial tau cytopathologies in progressive supranuclear palsy. *Acta Neuropathol*. Sep 2023;146(3):395-414. doi:10.1007/s00401-023-02604-x

3. Hoglinger GU, Respondek G, Stamelou M, et al. Clinical diagnosis of progressive supranuclear palsy: The movement disorder society criteria. *Mov Disord*. Jun 2017;32(6):853-864. doi:10.1002/mds.26987

4. Respondek G, Stamelou M, Kurz C, et al. The phenotypic spectrum of progressive supranuclear palsy: a retrospective multicenter study of 100 definite cases. *Mov Disord*. Dec 2014;29(14):1758-66. doi:10.1002/mds.26054

5. Respondek G, Kurz C, Arzberger T, et al. Which ante mortem clinical features predict progressive supranuclear palsy pathology? *Mov Disord*. Jul 2017;32(7):995-1005. doi:10.1002/mds.27034

6. Huang SY, Chen SF, Cui M, et al. Plasma Biomarkers and Positron Emission Tomography Tau Pathology in Progressive Supranuclear Palsy. *Mov Disord*. Apr 2023;38(4):676-682. doi:10.1002/mds.29339

7. Olfati N, Ghodsi H, Bayram E, Litvan I. Why Therapeutic Trials Fail in Primary Tauopathies. *Mov Disord*. Apr 2023;38(4):545-550. doi:10.1002/mds.29322

8. Vacchi E, Lazzarini E, Pinton S, et al. Tau protein quantification in skin biopsies differentiates tauopathies from alpha-synucleinopathies. *Brain*. Aug 27 2022;145(8):2755-2768. doi:10.1093/brain/awac161

9. Baiardi S, Quadalti C, Mammana A, et al. Diagnostic value of plasma p-tau181, NfL, and GFAP in a clinical setting cohort of prevalent neurodegenerative dementias. *Alzheimers Res Ther*. Oct 12 2022;14(1):153. doi:10.1186/s13195-022-01093-6

10. Rodriguez-Leyva I, Chi-Ahumada EG, Carrizales J, et al. Parkinson disease and progressive supranuclear palsy: protein expression in skin. *Ann Clin Transl Neurol*. Mar 2016;3(3):191-9. doi:10.1002/acn3.285

11. Tabaton M, Cammarata S, Mancardi GL, Cordone G, Perry G, Loeb C. Abnormal tau-reactive filaments in olfactory mucosa in biopsy specimens of patients with probable Alzheimer's disease. *Neurology*. Mar 1991;41(3):391-4. doi:10.1212/wnl.41.3.391

12. Yamagishi M, Ishizuka Y, Seki K. Pathology of olfactory mucosa in patients with Alzheimer's disease. *Ann Otol Rhinol Laryngol*. Jun 1994;103(6):421-7. doi:10.1177/000348949410300601

13. Hattori H, Matsumoto M, Iwai K, et al. The tau protein of oral epithelium increases in Alzheimer's disease. *J Gerontol A Biol Sci Med Sci*. Jan 2002;57(1):M64-70. doi:10.1093/gerona/57.1.m64

14. Guo Z, Tian C, Shi Y, et al. Blood-based CNS regionally and neuronally enriched extracellular vesicles carrying pTau217 for Alzheimer's disease diagnosis and differential diagnosis. *Acta Neuropathol Commun*. Mar 5 2024;12(1):38. doi:10.1186/s40478-024-01727-w

15. Tian C, Stewart T, Hong Z, et al. Blood extracellular vesicles carrying synaptic function- and brain-related proteins as potential biomarkers for Alzheimer's disease. *Alzheimers Dement*. Mar 2023;19(3):909-923. doi:10.1002/alz.12723

16. Yan S, Jiang C, Janzen A, et al. Neuronally Derived Extracellular Vesicle alpha-Synuclein as a Serum Biomarker for Individuals at Risk of Developing Parkinson Disease. *JAMA Neurol*. Jan 1 2024;81(1):59-68. doi:10.1001/jamaneurol.2023.4398

17. Shi M, Liu C, Cook TJ, et al. Plasma exosomal alpha-synuclein is likely CNS-derived and increased in Parkinson's disease. *Acta Neuropathol*. Nov 2014;128(5):639-650. doi:10.1007/s00401-014-1314-y

18. Ha D, Yang N, Nadithe V. Exosomes as therapeutic drug carriers and delivery vehicles across biological membranes: current perspectives and future challenges. *Acta Pharm Sin B*. Jul 2016;6(4):287-96. doi:10.1016/j.apsb.2016.02.001

19. Li F, Xie XY, Sui XF, Wang P, Chen Z, Zhang JB. Profile of Pathogenic Proteins and MicroRNAs in Plasma-derived Extracellular Vesicles in Alzheimer's Disease: A Pilot Study. *Neuroscience*. Apr 15 2020;432:240-246. doi:10.1016/j.neuroscience.2020.02.044

20. Manolopoulos A, Delgado-Peraza F, Mustapic M, et al. Comparative assessment of Alzheimer's disease-related biomarkers in plasma and neuron-derived extracellular vesicles: a nested case-control study. *Front Mol Biosci*. 2023;10:1254834. doi:10.3389/fmolb.2023.1254834

21. Meloni M, Agliardi C, Guerini FR, et al. Oligomeric α-synuclein and tau aggregates in NDEVs differentiate Parkinson's disease from atypical parkinsonisms. *Neurobiol Dis*. Jan 2023;176:105947. doi:10.1016/j.nbd.2022.105947

22. Wang Z, Zheng Y, Cai H, et al. Abeta1-42-containing platelet-derived extracellular vesicle is associated with cognitive decline in Parkinson's disease. *Front Aging Neurosci*. 2023;15:1170663. doi:10.3389/fnagi.2023.1170663

23. Yu Z, Zheng Y, Cai H, et al. Molecular beacon–based detection of circulating microRNA-containing extracellular vesicle as an α-synucleinopathy biomarker. *Science Advances*. May 17 2024;10(20):eadl6442. doi:10.1126/sciadv.adl6442

24. Postuma RB, Berg D, Stern M, et al. MDS clinical diagnostic criteria for Parkinson's disease. *Mov Disord*. Oct 2015;30(12):1591-601. doi:10.1002/mds.26424

25. Ali F, Martin PR, Botha H, et al. Sensitivity and Specificity of Diagnostic Criteria for Progressive Supranuclear Palsy. *Mov Disord*. Aug 2019;34(8):1144-1153. doi:10.1002/mds.27619

26. Hall S, Öhrfelt A, Constantinescu R, et al. Accuracy of a panel of 5 cerebrospinal fluid biomarkers in the differential diagnosis of patients with dementia and/or parkinsonian disorders. *Arch Neurol*. Nov 2012;69(11):1445-52. doi:10.1001/archneurol.2012.1654

27. Wagshal D, Sankaranarayanan S, Guss V, et al. Divergent CSF τ alterations in two common tauopathies: Alzheimer's disease and progressive supranuclear palsy. *Journal of neurology, neurosurgery, and psychiatry*. Mar 2015;86(3):244-50. doi:10.1136/jnnp-2014-308004

28. Saijo E, Metrick MA, 2nd, Koga S, et al. 4-Repeat tau seeds and templating subtypes as brain and CSF biomarkers of frontotemporal lobar degeneration. *Acta Neuropathol*. Jan 2020;139(1):63-77. doi:10.1007/s00401-019-02080-2

29. Dellarole IL, Vacchi E, Ruiz-Barrio I, et al. Tau seeding activity in skin biopsy differentiates tauopathies from synucleinopathies. *NPJ Parkinsons Dis*. Jun 15 2024;10(1):116. doi:10.1038/s41531-024-00728-9

30. Zhang Y, Wu KM, Yang L, Dong Q, Yu JT. Tauopathies: new perspectives and challenges. *Mol Neurodegener*. Apr 7 2022;17(1):28. doi:10.1186/s13024-022-00533-z

31. Lukic MJ, Respondek G, Kurz C, et al. Long-Duration Progressive Supranuclear Palsy: Clinical Course and Pathological Underpinnings. *Ann Neurol*. Oct 2022;92(4):637-649. doi:10.1002/ana.26455

32. Schirinzi T, Sancesario GM, Di Lazzaro G, et al. Clinical value of CSF amyloid-beta-42 and tau proteins in Progressive Supranuclear Palsy. *J Neural Transm (Vienna)*. Sep 2018;125(9):1373-1379. doi:10.1007/s00702-018-1893-1

33. Urakami K, Wada K, Arai H, et al. Diagnostic significance of tau protein in cerebrospinal fluid from patients with corticobasal degeneration or progressive supranuclear palsy. *J Neurol Sci*. Jan 15 2001;183(1):95-8. doi:10.1016/s0022-510x(00)00480-9

34. Blair LJ, Frauen HD, Zhang B, et al. Tau depletion prevents progressive blood-brain barrier damage in a mouse model of tauopathy. *Acta Neuropathol Commun*. Jan 31 2015;3:8. doi:10.1186/s40478-015-0186-2

35. Norman M, Ter-Ovanesyan D, Trieu W, et al. L1CAM is not associated with extracellular vesicles in human cerebrospinal fluid or plasma. *Nat Methods*. Jun 2021;18(6):631-634. doi:10.1038/s41592-021-01174-8

36. Nogueras-Ortiz CJ, Eren E, Yao P, et al. Single-extracellular vesicle (EV) analyses validate the use of L1 Cell Adhesion Molecule (L1CAM) as a reliable biomarker of neuron-derived EVs. *J Extracell Vesicles*. Jun 2024;13(6):e12459. doi:10.1002/jev2.12459

37. Yan S, Zhang W, Li X, et al. Single extracellular vesicle detection assay identifies membrane-associated α-synuclein as an early-stage biomarker in Parkinson's disease. *Cell Rep Med*. Mar 18 2025;6(3):101999. doi:10.1016/j.xcrm.2025.101999

38. Wang X, Zheng Y, Cai H, et al. α-Synuclein species in plasma neuron-derived extracellular vesicles as biomarkers for iRBD. *Ann Clin Transl Neurol*. Nov 2024;11(11):2891-2903. doi:10.1002/acn3.52200

Figure legends

Figure 1 Characteristics of EVs. (**A**) EV structure revealed by TEM showed a diameter ≈ 100 nm. (**B**) Western blot validation of NDEV specificity and cargo enrichment. (**C**) NTA showed a population of EVs with a peak ≈ 100 nm in PSP. (**D**) NTA showed a population of EVs with a peak ≈ 100 nm in PD. (**E**) NTA showed a population of EVs with a peak ≈ 100 nm in HCs. (**F**) Total concentration of EVs of all particle sizes in PSP, PD and HCs plasma.

Figure 2 Nano-scale flow cytometry analysis of EVs in plasma. (**A-F**) Example histograms showing populations of tau-species-containing NDEVs in the reference plasma, the IgG isotype control, and the EV-depleted plasma control. (**G-L**) The levels of tau-species-containing NDEVs among the reference plasma, the IgG isotype control, and the EV-depleted plasma control. (**M-R**) linearity in different dilutions of EV plasma samples.

Figure 3 Tau-species-containing NDEVs in the discovery cohort. (**A-F**) The concentrations of tau, 4R tau, ptau181, ptau217, ptau231, and ptau396-containing NDEVs in plasma of PSP, PD, and HCs. (**G-L**) The ratios of tau-species positive NDEVs to tau-species positive EVs in plasma of PSP, PD, and HCs. (**M-N**) ROC curves of plasma tau-species-containing NDEVs for discriminating patients with PSP and HCs. (**O-P**) ROC curves of plasma tau-species-containing NDEVs for discriminating patients with PSP and PD.

Figure 4 Tau-species-containing NDEVs in the validation cohort. (**A-F**) The concentrations of tau, 4R tau, ptau181, ptau217, ptau231, and ptau396-containing NDEVs in plasma of PSP, PD, and HCs. (**G-L**) The ratios of tau-species positive NDEVs to tau-species positive EVs in plasma of PSP, PD, and HCs. (**M-N**) ROC curves of plasma tau-species-containing NDEVs for discriminating patients with PSP and HCs. (**O-P**) ROC curves of plasma tau-species-containing NDEVs for discriminating patients with PSP and PD.

Figure 5 Tau-species-containing NDEVs between early-stage PSP and early-stage PD patients. (**A-F**) The concentrations of tau, 4R tau, ptau181, ptau217, ptau231, and ptau396-containing NDEVs in plasma of early-stage PSP and early-stage PD patients. (**G-H**) ROC curves of plasma tau-species-containing NDEVs for discriminating patients with early-stage PSP and early-stage PD patients.

Table 1 Demographic and clinical features in the discovery and validation cohorts

Data	Discovery cohort				Validation cohort			
	PSP (n = 40)	**PD (n = 36)**	**HCs (n = 31)**	***P***	**PSP (n = 30)**	**PD (n = 27)**	**HCs (n = 24)**	***P***
Sex, male/female	27/13	23/13	21/10	0.929[a]	17/13	13/14	11/13	0.696[a]
Age, years[b]	68 (45–77)	67 (56–76)	66 (56–75)	0.704[c]	64 (54–78)	67 (56–77)	68.5 (55–75)	0.733[c]
Onset age, years[b]	64.5 (43–73)	60 (50–70)	/	**0.016[d]**	62 (53–77)	61 (49–74)	/	0.631[d]
Duration, years[b]	3 (0.5–10)	6 (1–16)	/	**<0.001[d]**	3 (0.83–8)	5 (1–13)	/	**0.018[d]**
MMSE[b]	23.5 (9–30)	27 (17–30)	/	**<0.001[d]**	24 (12–30)	27 (23–30)	/	**<0.001[d]**
MoCA[e]	16.68 ± 5.90	21 ± 5.67	/	**0.002[f]**	18.37 ± 5.88	23 ± 4.65	/	**0.002[f]**
MDS-UPDRS III[e]	42.90 ± 17.04	39.22 ± 12.86	/	0.296[f]	45.9 ± 18.52	36.48 ± 14.28	/	**0.038[f]**
Hoehn-Yahr[b]	/	3 (1–5)	/	/	/	3 (1.5–4)	/	/

PSP = progressive supranuclear palsy; PD = Parkinson's disease; HCs = healthy controls; MMSE = Mini-Mental State Examination; MoCA = Montreal Cognitive Assessment; MDS-UPDRS III = Movement Disorder Society Unified Parkinson's Disease Rating Scale Part III.

[a]Pearson's chi-squared test.

[b]Data are expressed as median (range).

[c]Kruskal-Wallis test followed by pairwise Mann-Whitney U test.

[d]Mann-Whitney U test.

[e]Data are expressed as mean ± standard deviation.

[f]Unpaired t test.

Table 2 Parameters of the multivariable logistic regression models for differentiating PSP from HCs and PD

	PSP versus HC Model			PSP versus PD Model		
Variables	**B**	***P* value**	**OR (95% CI)**	**B**	***P* value**	**OR (95% CI)**
Intercept	–3.535	0.008	/	–4.437	0.002	/
Tau+ NDEVs	1.619	0.031	5.048 (1.164–21.893)	1.386	0.025	4.000 (1.188–13.468)
4R tau+ NDEVs	1.841	0.016	6.303 (1.412–28.133)	2.54	0.002	12.686 (2.593–62.067)
ptau 181+ NDEVs	1.272	0.082	3.570 (0.850–15.000)	0.322	0.545	1.380 (0.486–3.924)
ptau 217+ NDEVs	1.27	0.127	3.562 (0.697–18.206)	3.104	0.034	22.288 (1.261–393.803)
ptau 231+ NDEVs	0.772	0.245	2.165 (0.589–7.953)	0.811	0.185	2.249 (0.679–7.448)
ptau 396+ NDEVs	0.055	0.929	1.057 (0.313–3.564)	-0.283	0.462	0.753 (0.354–1.603)

NDEVs = neuron-derived extracellular vesicles; PSP = progressive supranuclear palsy; HC = healthy control; PD = Parkinson's disease; OR = odds ratio; CI = confidence interval.

Table 3 Demographic and clinical features of early-stage PSP and PD

Data	early-stage PSP (n = 43)	early-stage PD (n = 18)	*P*
Sex, male/female	25/18	6/12	0.077[a]
Age, years[b]	66.26 ± 7.09	65.72 ± 6.17	0.782[c]
Onset age, years[b]	64.04 ± 7.03	63.42 ± 6.27	0.746[c]
Duration, years[d]	2 (0.5–3)	2.25 (1–3)	0.847[e]
MMSE[d]	24 (9–30)	27 (17–30)	0.005[e]
MoCA[b]	17.02 ± 6.30	22.28 ± 6.15	0.004[c]
MDS-UPDRS III[b]	42.67 ± 19.50	32.11 ± 14.84	0.044[c]
Hoehn-Yahr[d]	/	2 (1–4)	/

PSP = progressive supranuclear palsy; PD = Parkinson's disease; MMSE = Mini-Mental State Examination; MoCA = Montreal Cognitive Assessment; MDS-UPDRS III = Movement Disorder Society Unified Parkinson's Disease Rating Scale Part III.

[a]Pearson's chi-squared test.

[b]Data are expressed as mean ± standard deviation.

[c]Unpaired t test.

[d]Data are expressed as median (range).

[e]Mann-Whitney U test.

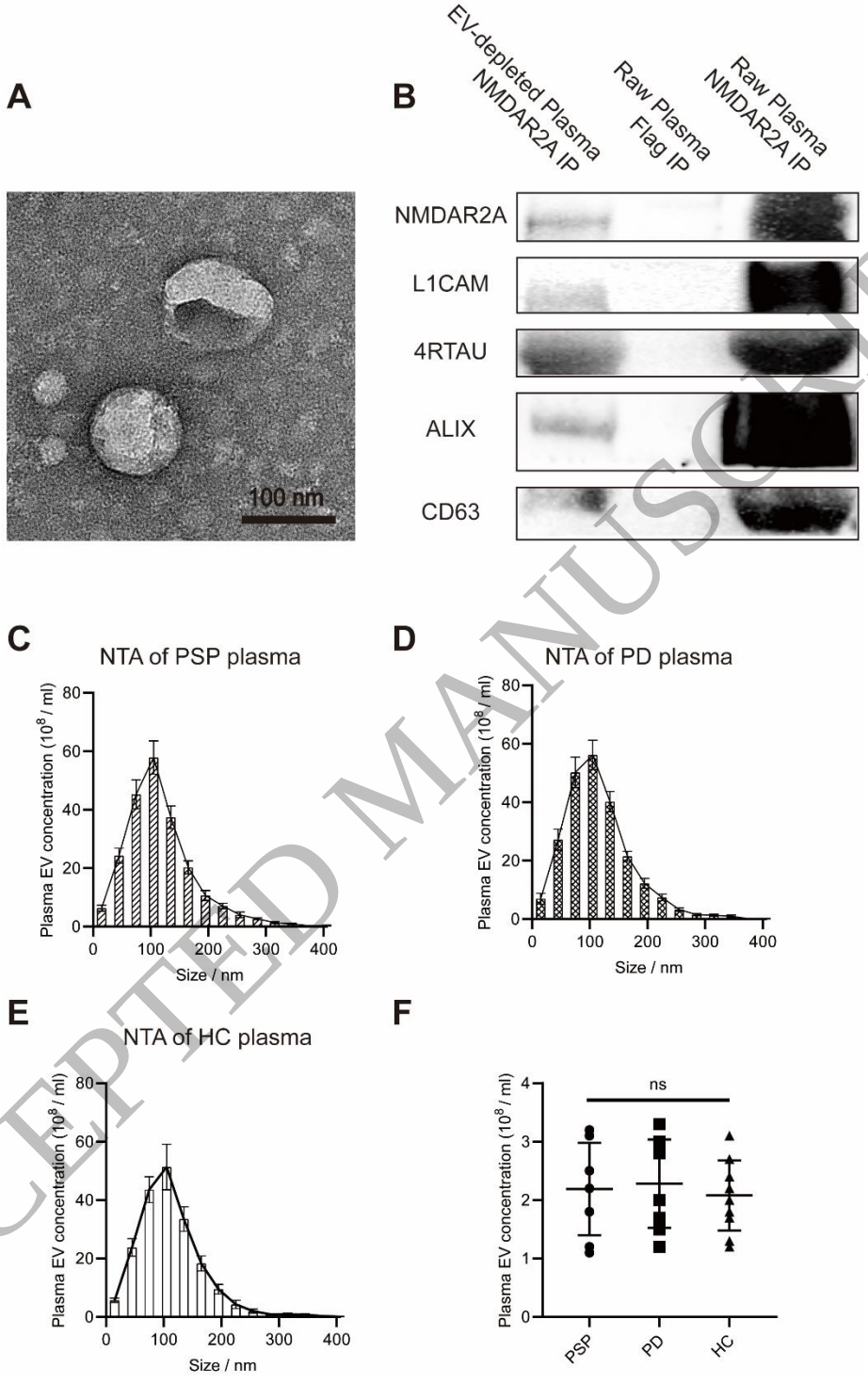

Figure 1
144x229 mm (x DPI)

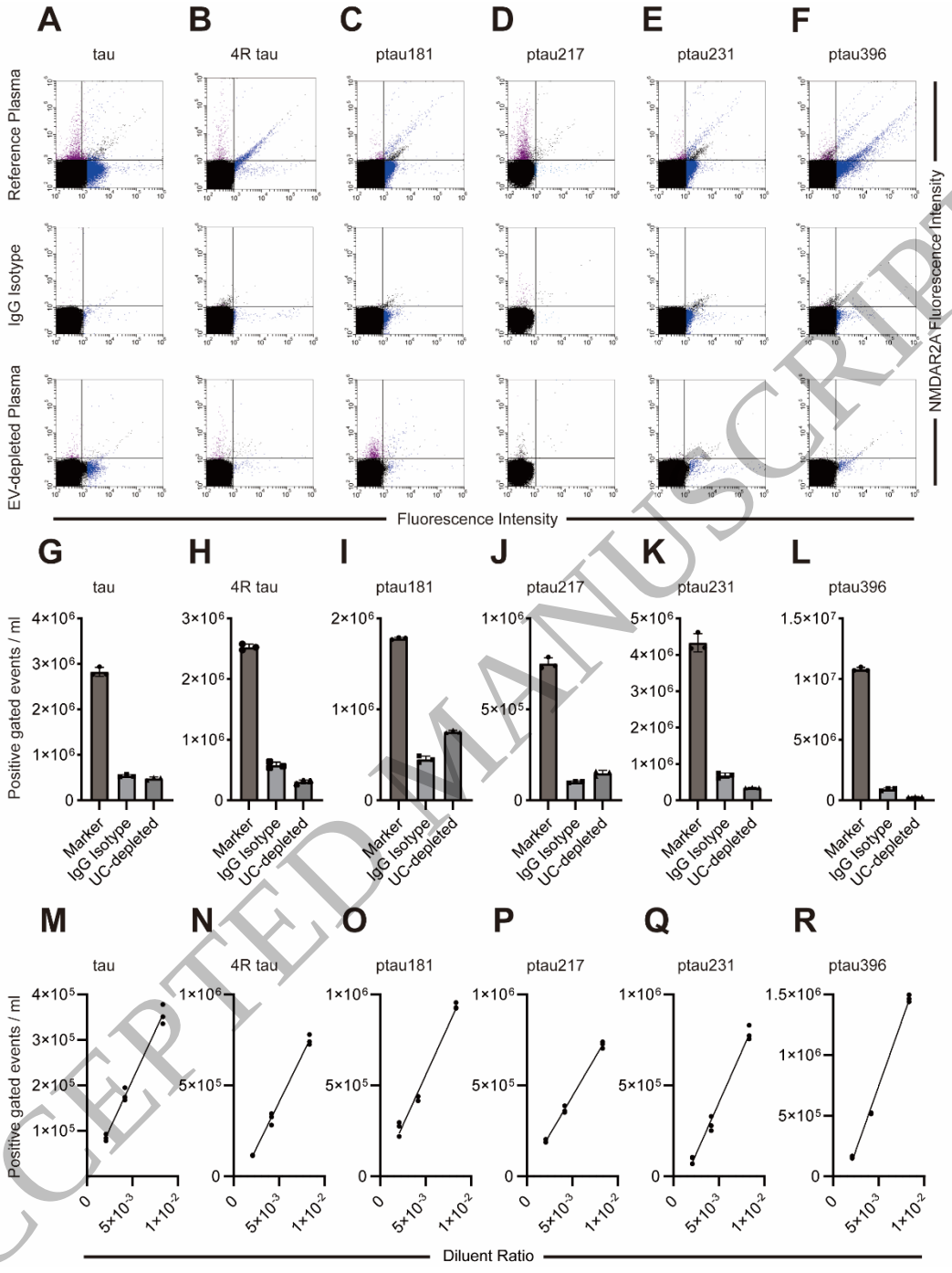

Figure 2
165x219 mm (x DPI)

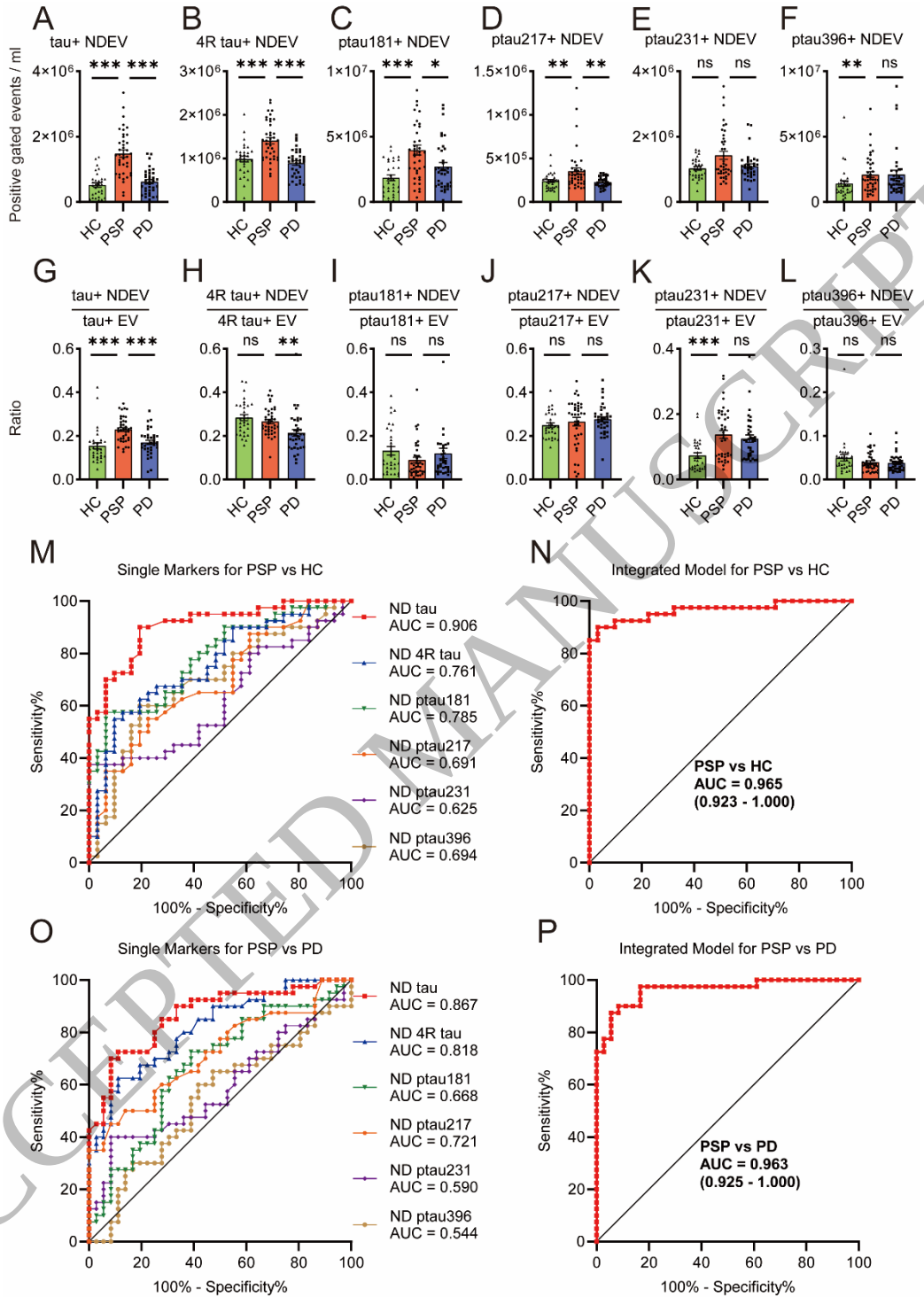

Figure 3
162x229 mm (x DPI)

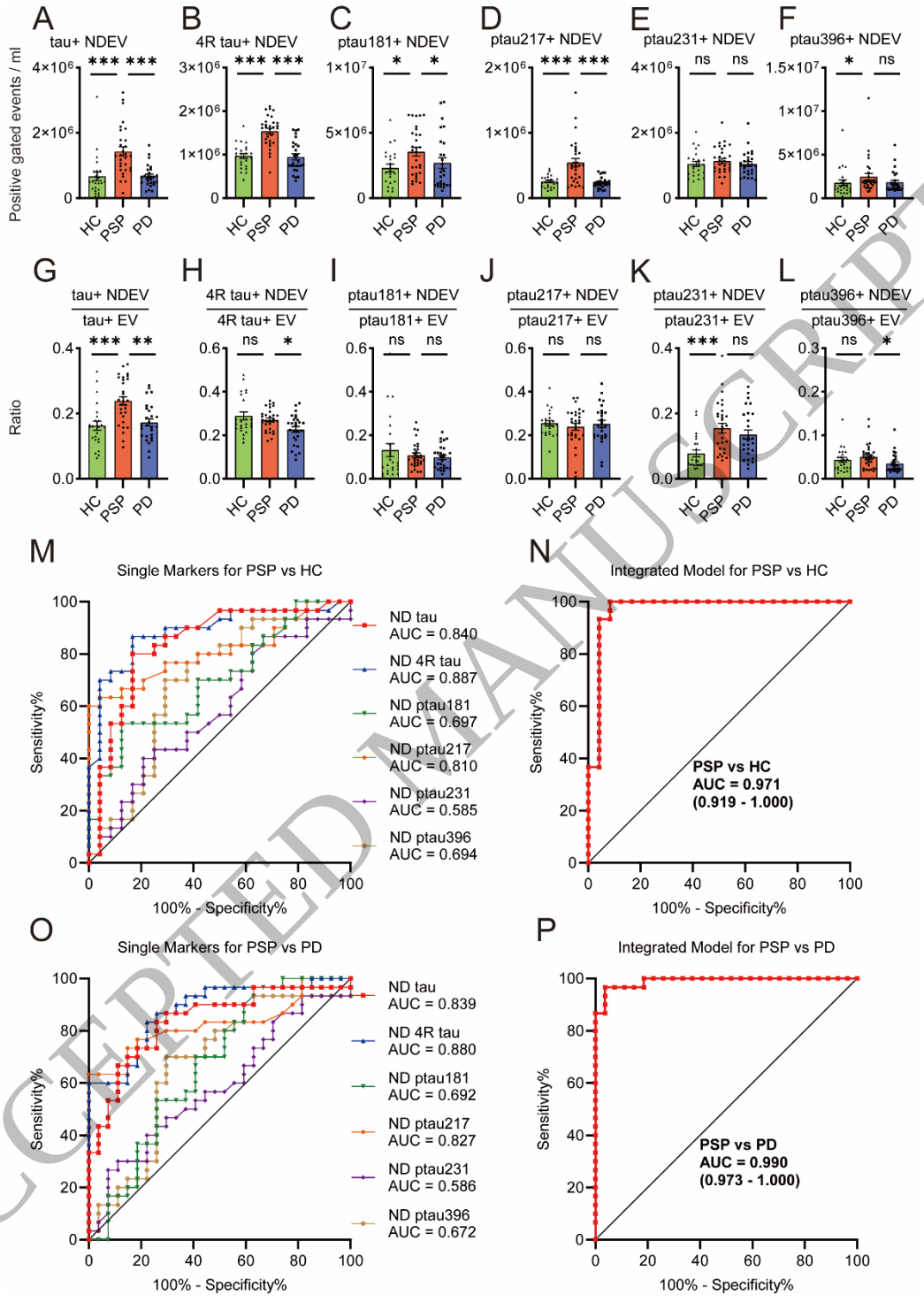

Figure 4
162x229 mm (x DPI)

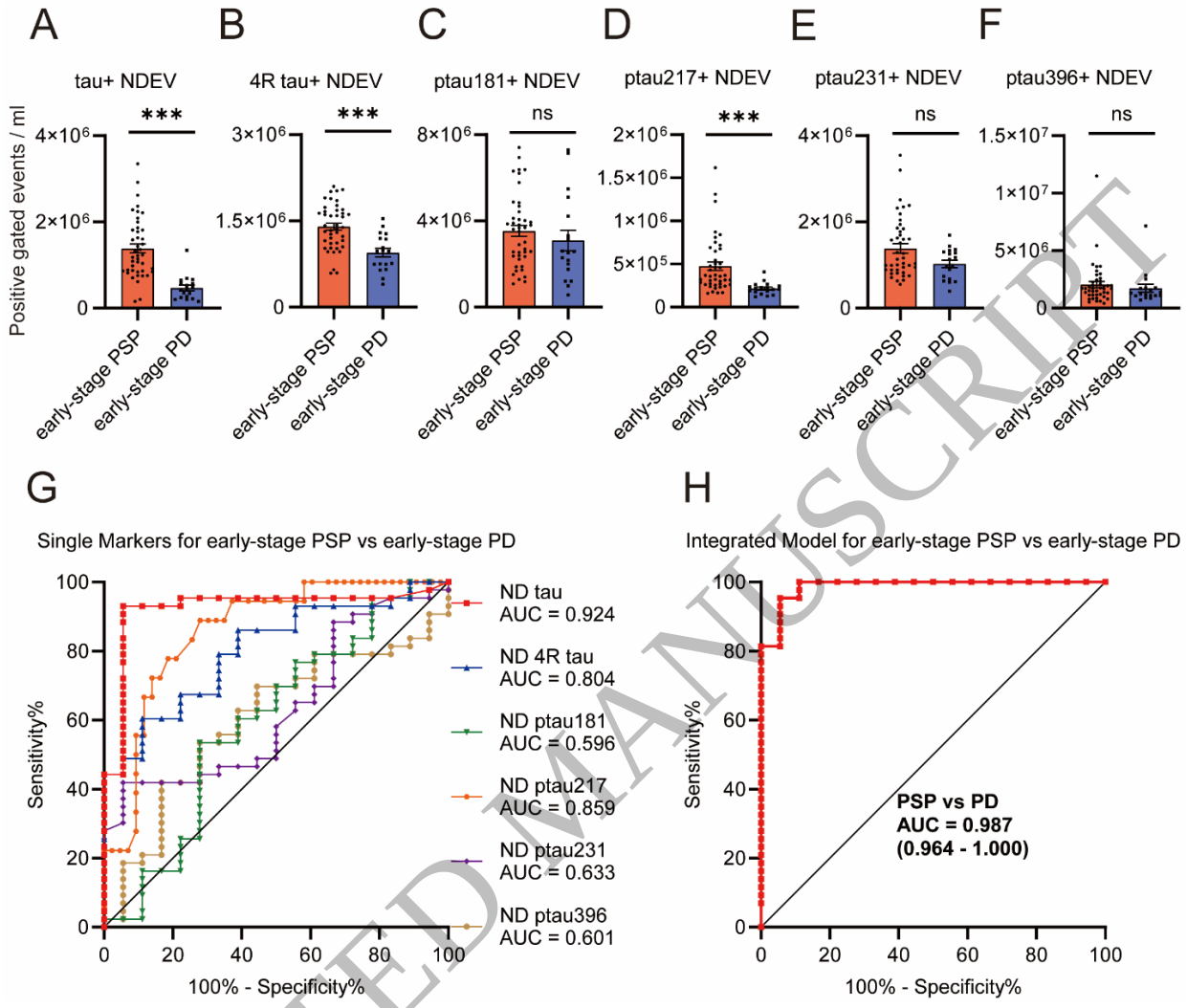

Figure 5
165x139 mm (x DPI)